Parasitol Res (2012) 111:2301–2309
DOI 10.1007/s00436-012-3084-6

ORIGINAL PAPER

The neuromuscular system in continuously swimming cercariae from Belarus. II Echinostomata, Gymnocephala and Amphistomata

Oleg O. Tolstenkov · Ludmila N. Akimova · Nadezhda B. Terenina · Margaretha K. S. Gustafsson

Received: 7 August 2012 / Accepted: 9 August 2012 / Published online: 2 September 2012

Abstract The neuromuscular system in cercariae of *Moliniella anceps*, *Echinostoma revolutum*, *Cathaemasia hians*, *Psilochasmus oxyurus*, *Sphaeridiotrema globulus*, *Paramphistomum cervi* and *Diplodiscus subclavatus* was studied with immunocytochemical methods and confocal scanning laser microscopy. The patterns of F-actin in the musculature, 5-HT immunoreactive (IR), FMRFamide-IR neuronal elements and α-tubulin-IR sensory receptors were investigated. The general patterns of musculature, 5-HT- and FMRFamide-IR neuronal elements in the 12 species studied here and in paper I are similar to those observed in other cercariae and reflect the morphology of the groups. The musculature of the tail shows variations which are related to the different strategies of host finding. In the Echinostomatoidea and Paramphistomoidea, the striated musculature of the tail is well developed compared to that in the Xiphidiocercariae. Specialized muscle fibres were found in *S. globulus*, which are able to change the shape of the tail. Nine of the species studied have seven paired 5-HT-IR neurons in the body, and two species have eight. No correlation between the body size and the number of 5-HT-IR neurons was observed. However, the size of the neurons followed the body size. The number of 5-HT-IR neurons in the brain ganglia increased from the primitive to the advanced forms. The number of FMRFamide-IR transverse commissures in the body correlates with the size of the cercariae. Regardless of the differences in the second intermediate host, the distribution of α-tubulin-IR sensory receptors shows a high degree of conformity in all species except in *P. cervi*, which encysts on plants.

O. O. Tolstenkov (✉) · N. B. Terenina
Centre of Parasitology of A. N. Severtsov Institute of Ecology and Evolution, Russian Academy of Sciences,
Leninsky prospect, 33,
Moscow 119071, Russia
e-mail: otolo@rambler.ru

L. N. Akimova
Laboratory of Parasitology,
State Scientific and Production Amalgamation,
"The Scientific and Practical Center for Bioresources",
27 Akademicheskaya Street,
Minsk 220072, Republic of Belarus

M. K. S. Gustafsson
Department of Biosciences, Åbo Akademi University,
20520 Åbo, Finland

Introduction

Cercariae with a continuously swimming mode include several morphological groups. Among them are the highly specialized plagiorchid Xiphidiocercariae which were described in paper I (Tolstenkov et al. 2012c). In the present paper, we continue our comparative study of the morphology of the neuromuscular system (NMS) in trematode cercariae (see Tolstenkov et al. 2012a, b, c). This time we focus on three primitive groups.

We describe the NMS in five species of Echinostomatoidea Looss, 1899 *Moliniella anceps* Molin, 1859; *Echinostoma revolutum* Fröhlich, 1802 (Echinostomatidae Looss, 1899); *Cathaemasia hians* Rudolphi, 1809 (Cathaemasiidae Fuhrmann, 1928); *Psilochasmus oxyurus* Creplin, 1825; *Sphaeridiotrema globulus* Rudolphi, 1814 (Psilostomidae Looss, 1900) and two species of Paramphistomoidea Fischoeder, 1901 *Paramphistomum cervi* Zeder, 1790 (Paramphistomidae Fischoeder, 1901) and *Diplodiscus subclavatus* Pallas, 1760 (Diplodiscidae Cohn, 1904). Based on the major morphological features, such as the presence and position of suckers or armed collar, Dawes (1946) refers representatives of the families Echinostomatidae and Cathaemasiidae to the groups Echinostomata or Echinostome cercaria, family Psilostomidae to the group Gymnocephala cercaria and the families Paramphistomidae and

Diplodiscidae to the groups Amphistomata or Amphistome cercaria.

All these cercariae possess well-developed organs of digestion and many flame cells. They lack penetration glands and stylet. Most of them are large. *P. oxyurus* and *D. subclavatus* are among the biggest freshwater cercaria known so far. They swim slowly and after a short period of active life encyst on different substrates (Dawes 1946). These trematode species are abundant in the ecosystems and frequently cause diseases in water fowl, cattle and sometimes in humans (Keiser and Utzinger 2009; Herrmann and Sorensen 2011).

The organisation of the NMS and the distribution of serotonin and a few neuropeptides have been studied in three species of Echinostomatidae cercariae by Richard et al. (1989); Šebelová et al. (2004) and Terenina et al. (2006). A preliminary study of one species of Psilostomidae was performed by Tolstenkov et al. (2008). Several studies of the chaetotaxy in family Echinostomatidae and Paramphistomidae have been performed (see Konstadinova 1999; Albaret et al. 1987). As far as we know, the NMS in cercariae from the families Cathaemasiidae and Diplodiscidae has never before been described.

Materials and methods

Samples of snails *Stagnicola palustris* Müller, 1774; *Radix ampla* Hartmann, 1821; *Planorbis planorbis* Linnaeus, 1758; *Bithynia leachi* Sheppard, 1823 and *Bithynia tentaculata* Linnaeus, 1758 were collected in the littoral zone of Lake Naroch and identified at the Scientific and Research Centre "Naroch biological station named after G.G. Vinberg" of the Belarusian State University, Republic of Belarus, in July 2010–2011. The larval stages were identified according to Szidat (1936, 1957); Ginetsinskaya and Dobrovolsky (1964); Bihovskaya-Pavlovskaya and Kulakova (1971); Belyakova (1978); Grabda-Kazubska et al. (1990) and Kanev (1994). The mollusc nomenclature was applied after Glöer (2002).

Specimens of cercariae *M. anceps* were recovered from *S. palustris*, cercariae *E. revolutum* from *R. ampla*, cercariae *C. hians*, *P. cervi* and *D. subclavatus* from *P. planorbis*, cercariae *P. oxyurus* from *B. leachi*, cercariae *S. globulus* from *B. tentaculata*. For the methods descriptions, see Tolstenkov et al. (2012a).

Results

The patterns of staining with TRITC-labelled phalloidin

The cercariae fall into different size classes (Table 1). In *M. anceps* cercariae, staining with TRITC-conjugated phalloidin revealed a body wall consisting of a well-organised outer layer of regularly distributed circular muscle fibres, an intermediate layer of longitudinal muscle fibres, forming pairs and running straight, and an inner layer of regularly distributed single diagonal muscle fibres (Fig. 1a). The diagonal layer is absent in the posterior part of the body. Dorsoventral fibres were also observed. In the constriction region of the armed disc in the head, strong transverse muscle fibres were observed. From the centre of the armed disc, many muscle fibres radiate outwards (Fig. 1b). The oral sucker has an outer and an inner layer of circular and longitudinal muscle fibres, and in addition a well-developed layer of radial fibres (Fig. 1b). Longitudinal and radial muscle fibres form the musculature of the pharynx. In the walls of the oesophagus and intestine, single circular and many longitudinal fibres occur. The ventral sucker is formed by circular, longitudinal and radial fibres and is attached to the body wall by single longitudinal muscle fibres. The excretory ducts are lined by a few longitudinal and circular muscle fibres, which become denser in the terminal part. The bladder is cylindrical (Fig. 1c). The tail contains an outer circular layer of single smooth muscle fibres, four narrow bands of smooth muscle fibres (2.2 μm wide) and striated muscle fibres organised into the four bundles (17–19 μm wide; Fig. 1a).

In *E. revolutum* and *C. hians* cercariae, the phalloidin staining was unsuccessful, although the major features of the musculature could be observed. They are similar to those in *M. anceps* cercariae. The general pattern of phalloidin-stained F-actin filaments in the musculature of *P. oxyurus*

Table 1 Size of cercariae

	Body		Tail		Body wall muscle fibres		
	Length	Width	Length	Width	Circular	Longitudinal	Diagonal
M. anceps	623.1	285.5	994.5	94.2	0.5	0.9	0.9
E. revolutum	280.9	123.7	396.7	47.7	–	–	–
C. hians	470.0	201.2	680.4	73.8	–	–	–
P. oxyurus	739.7	363.1	802.0	94.9	0.8	0.9	1.1
S. globulus	142.2	88.0	162.0	33.5	0.5	0.6	0.6
P. cervi	240.4	226.9	798.7	77.5	0.5	0.7	0.9
D. subclavatus	727.0	319.9	1,141.1	139.4	0.5	0.8	0.9

Diameter of single muscle fibres in the body (in micrometer)

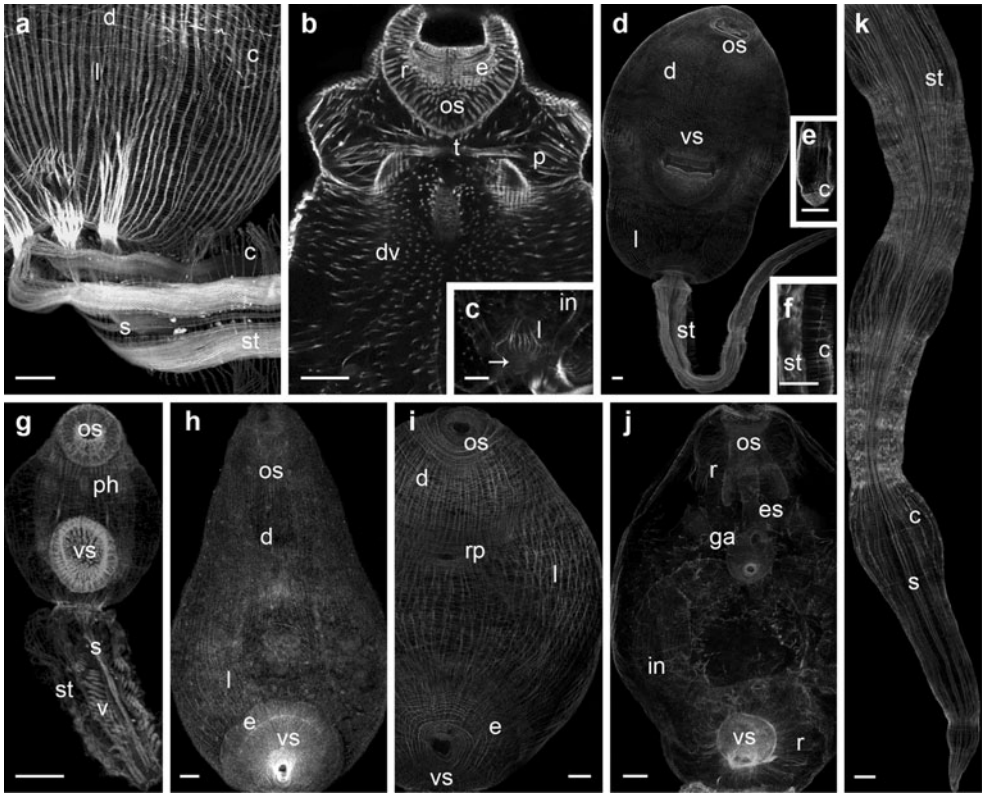

Fig. 1 **a**–**k** Confocal scanning laser micrographs of the pattern of TRITC-phalloidin-conjugated F-actin in cercariae. *Bar*=20 μm. **a** Max projection of *M. anceps* showing the musculature of the body wall and the tail. **b** Optical section *M. anceps* showing the musculature of the oral sucker and the armed disc. **c** Optical section of *M. anceps* showing the musculature of the bladder (*arrow*) and intestine. **d** Max projection of *P. oxyurus* showing the musculature of the body wall, oral and ventral suckers and tail. **e** Max projection of the cap-like structure in the tip of the tail of *P. oxyurus*. **f** Max projection showing the musculature of the tail of *P. oxyurus*. **g** Max projection of *S. globulus* showing the musculature of the body wall, oral and ventral suckers and tail. **h** Max projection of *P. cervi* showing the musculature of the body wall and oral and ventral suckers. **i** Max projection of *D. subclavatus* showing the musculature of the body wall and oral and ventral suckers. **j** Optical section of *D. subclavatus* showing the musculature of the inner organs. **k** Max projection showing the musculature of the tail of *D. subclavatus*. *c* circular muscle fibres, *d* diagonal muscle fibres, *dv* dorsoventral muscle fibres, *e* equatorial muscle fibres, *es* oesophagus, *ga* genital atrium, *in* intestine, *l* longitudinal muscle fibres, *os* oral sucker, *p* parenchymal fibres, *ph* pharynx, *r* radial muscle fibres, *rp* reproductive pore, *s* smooth muscle fibres, *st* striated muscle fibres, *t* transverse muscle fibres, *v* specialized fibres on ventral side, *vs* ventral sucker

cercariae is similar to that in *M. anceps* (Fig. 1d). *P. oxyurus* cercariae lack an armed disc. Many dorsoventral muscle fibres were observed. The pharynx contains a layer of radial fibres. The oesophagus is comparatively short. In the tail, smooth muscle fibres (1.6 μm wide) and bundles of striated fibres (37 μm wide) occur. Pairs of circular, plaited muscle fibres (0.8 μm wide) occur regularly in the tail (Fig. 1f). In the posterior part of the tail, the striated muscle fibres bend towards the central axis of the tail. In the tip of the tail, dense circular fibres form a cap-like structure (Fig. 1e).

In the small *S. globulus* cercariae, the pattern of muscle fibres is similar to that in *P. oxyurus* (Fig. 1g). However, the single muscle fibres are thinner, and they are not so densely packed. The radial fibres in the oral and ventral suckers are sparsely distributed (Fig. 1g). The cercariae have a long oesophagus with a few circular and longitudinal muscle fibres. In the bulky tail, the smooth muscle fibres (0.8 μm wide) are located in the centre. On the dorsal side of the tail, the paired striated muscle fibres (0.6 μm wide) are diffusely distributed. The circular fibres in the tail do not form pairs. However, on the ventral side of the tail, the striated muscle fibres form a regular pattern with bands (0.8 μm wide) directed toward the central axis of the tail (Fig. 1g).

The general pattern and size of the muscle fibres in *P. cervi* cercariae are similar to those in the other cercariae studied. The enlarged ventral sucker is situated in the posterior part of the body (Fig. 1h). The pharynx is absent. In the tail, smooth muscle fibres (0.9 μm wide) and bands of striated muscle fibres (18 μm wide) occur. The striated muscle fibres narrow towards the tip of the tail and bend toward its central axis. In *D. subclavatus* cercariae, the pattern of the musculature is

similar to that in *P. cervi* cercariae. The oral sucker is represented by a thin-walled structure with two pockets consisting of circular, longitudinal and a few radial muscle fibres (Fig. 1i, j). The long oesophagus has a sphincter at its entrance. The genital atrium is spherical, formed by thin circular and longitudinal fibres and limited by two sphincters, one of them being the reproductive pore (Fig. 1i). The longitudinal muscle fibres of the body wall continue to the massive ventral sucker and attach to the opening of the sucker (Fig. 1i). Equatorial fibres are found at the surface of the ventral sucker (Fig. 1i). The tail contains smooth muscle bands (0.9 μm wide) and the bands of striated muscle fibres (22–40 μm wide; Fig. 1k).

The patterns of 5-HT immunoreactivity

In *M. anceps* cercariae, the 5-HT immunoreactive (5-HT-IR) nerve fibres form a symmetrical pattern and occur in the bilobed brain, the pair of main nerve cords (MCs) along the ventral surface, the pairs of lateral and dorsal minor cords and in the tail. The total number of 5-HT-IR neurons in the body is 16, and they are numbered in the figures (Fig. 2a, Table 2). Two pairs of neurons occur in the bilobed brain and six along each MC. Neuron pair number one is situated in the anterior lateral corner of each brain ganglion and sends processes towards the oral sucker. The second pair of neurons is situated at each end of the brain commissure. Neurons number three to five are situated along each MC

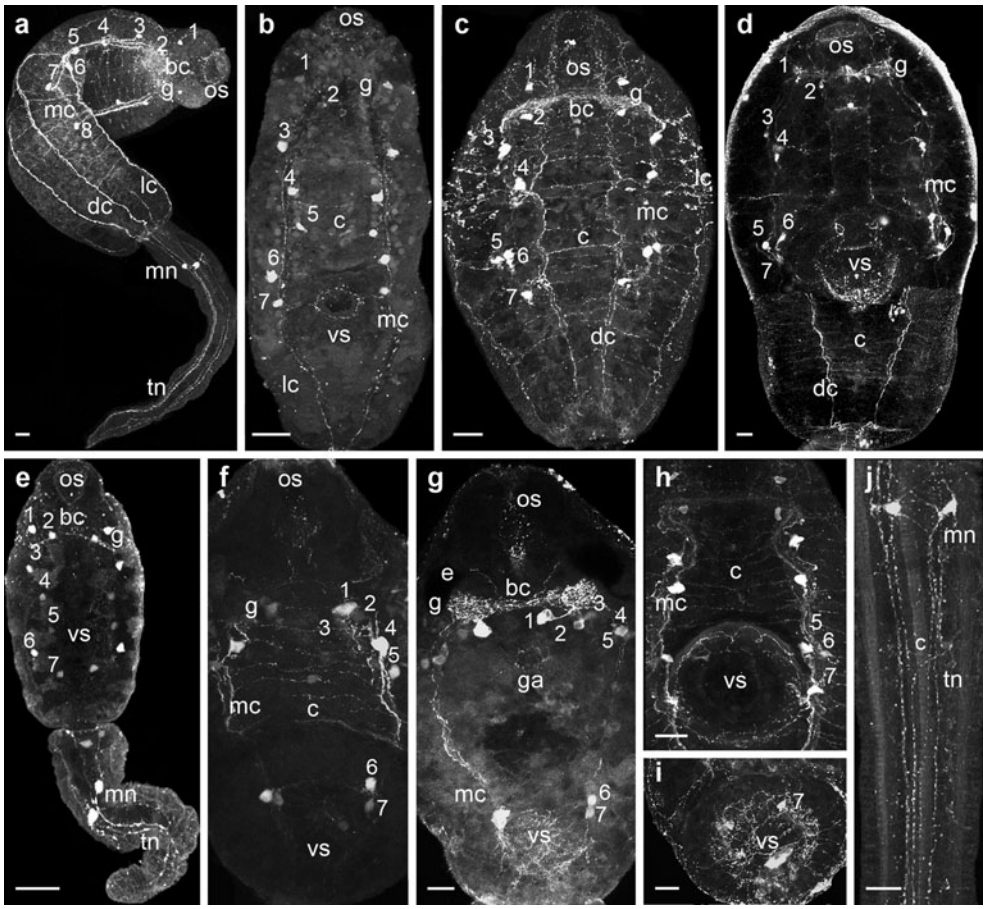

Fig. 2 **a**–**j** Confocal scanning laser micrographs of cercariae stained with anti-5-HT. *Bar*=20 μm. **a** Max projection showing the 5-HT-IR nervous system in *M. anceps*. The paired 5-HT-IR neurons are numbered. **b** Optical section showing the 5-HT-IR nervous system in the body of *E. revolutum*. **c** Optical section showing the 5-HT-IR nervous system in the body of *C. hians*. **d** Optical section showing the 5-HT-IR nervous system in the body of *P. oxyurus*. **e** Optical section of showing the 5-HT-IR nervous system in the body and tail of *S. globulus*. Note two multipolar neurons in the tail. **f** Optical section showing the 5-HT-IR nervous system of *P. cervi*. **g** Optical section showing the 5-HT-IR nervous system of *D. subclavatus*. Note the brain ganglia close to the eyes and the 5-HT-IR nerve ring around the genital atrium. **h** Optical section showing the 5-HT-IR main nerve cords with neurons in *E. revolutum*. Note the nerve ring in the ventral sucker. **i** Optical section showing the 5-HT-IR nervous system in the ventral sucker of *D. subclavatus*. **j** Optical section showing the two pairs of 5-HT-IR nerve cords in the tail of *E. revolutum*. Note the two multipolar neurons connected to both pairs of nerve cords. *bc* brain commissure, *c* commissure, *dc* dorsal nerve cord, *e* eye, *g* ganglion, *ga* genital atrium, *lc* lateral nerve cord, *mc* main nerve cord, *mn* multipolar neuron, *os* oral sucker, *tn* tail nerve, *vs* ventral sucker

between bilobed brain and the ventral sucker. Neurons number six to eight occur in the vicinity of the ventral sucker, sending nerves toward it. The longitudinal nerve cords are connected by 1 large brain commissure and 20 thin transverse commissures. From the ventral side of the bilobed brain, two 5-HT-IR nerve fibres extend towards the oral sucker (Fig. 2a). A pair of lateral anterior nerve cords also occurs. Rich 5-HT-IR plexuses were observed in the oral sucker, where they form a nerve ring, in the ventral sucker and at the distal end of the body. In the tail, two pairs of 5-HT-IR nerve cords run along the lateral sides. Two multipolar 5-HT-IR neurons occur in the first third of the tail. They are connected to both pairs of nerve cords (Fig. 2a).

In *E. revolutum* cercariae, the general pattern of the 5-HT immunostaining (IS) is similar to that of *M. anceps*, but the total number of neurons in the body is 14 (Fig. 2b). This species has two pairs of neurons in the bilobed brain and five neurons equally distributed along each MCs to the ventral sucker, where the last neuron sends the processes to its nerve ring. The 5-HT-IR neurons in *E. revolutum* are small (Table 2). The longitudinal cords are connected by one large brain commissure and ten thin transverse commissures.

In the cercariae of *C. hians*, the staining with anti-5-HT revealed a pattern similar to that in *E. revolutum*. The total number of neurons in the body is 14, two pairs in the bilobed brain, two along each MC between the brain ganglia and the ventral sucker and three in the vicinity of ventral sucker. The number of thin commissures in the body is 22–23 (Fig. 2c, h; Table 2). A 5-HT-IR nerve ring was observed in the ventral sucker (Fig. 2h). Figure 2j shows the two pairs of 5-HT-IR nerve cords and the two multipolar neurons in the tail of *C. hians*. In the tip of the tail, a 5-HT-IR nerve plexus was observed.

In *P. oxyurus* cercariae, the pattern of 5-HT-IS is similar to that in *C. hians.* An unpaired structure resembling a neuron was found in the middle of the pharynx. The number of thin commissures in the body is 25–26 (Fig. 2d, Table 2).

In *S. globulus* cercariae, the general pattern of the 5-HT IS is similar to that in *P. oxyurus*. However, the neurons are smaller. Two paired neurons occur in the bilobed brain, four along the MCs and the last pair in the vicinity of the ventral sucker, sending processes to it. No thin comissures are detected (Fig. 2e, Table 2).

In *P. cervi* cercariae, the pattern of 5-HT IS is similar to those in the other cercariae. The total number of neurons in the body is 14. Three pairs of neurons occur in bilobed brain, two at the beginning of each MC and two on either side of the distally situated big ventral sucker, close to its proximal surface. The number of thin commissures in the body is nine to ten (Fig. 2f, Table 2). In *D. subclavatus* cercariae, the pattern of 5-HT IS is similar to that in *P. cervi.* These cercariae have two large eyes. The 5-HT-IR nerve fibres of the bilobed brain reach close to the eyes (Fig. 2g). The neuronal cell bodies are large (Table 2). The genital opening is surrounded by a 5-HT-IR nerve ring (Fig. 2g). In the big ventral sucker, a rich plexus of 5-HT-IR nerves occurs (Fig. 2g, i). The controls were negative.

The patterns of FMRFamide immunoreactivity

In *M. anceps* cercariae, the nervous system stains strongly with anti-FMRFamide and follows the same general pattern as the 5-HT IS (Fig. 3a). The longitudinal cords are connected by a large brain commissure and a caudal commissure. Furthermore, 21 thin transverse commissures occur. Two FMRFamide-IR neurons (size 18.2×12.5 μm) occur on each side of the ventral sucker (Fig. 3a). In the tail, two pairs of FMRFamide-IR nerve cords run along the lateral sides. They are connected by transverse commissures. In the last third of the tail, two bipolar neurons (size 11.4×5.6 μm) were observed along the nerve cords (Fig. 3i). These neurons are not connected to both pairs of nerve cords.

In *E. revolutum* cercariae, the patterns of FMRFamide IS follows the 5-HT IS (Fig. 3b). However, the MCs contain multiple FMRFamide-IR nerve fibres.

In *C. hians* cercariae, the pattern of FMRFamide-IR nervous system is similar to that in *M. anceps*. In the posterior end of the body, a rich nerve plexus and six neurons (size 10.6×4.5 μm) were observed, three on each side of the bladder (Fig. 3c, inset). In *C. hians*, two FMRFamide-IR neurons (size 9.6×3.5 μm) are located in the first third of the tail (Fig. 3c).

In *P. oxyurus* cercariae, the FMRFamide IS follows the pattern of the 5-HT IS. Twenty-two to 23 thin transverse commissures connecting the MCs were observed. In the vicinity of the excretory bladder, a rich plexus of FMRFamide-IR nerves occurs (Fig. 3d). Both the oral and the ventral suckers are well innervated by FMRFamide-IR nerves.

Table 2 The number (*N*) and size (in micrometer) of 5-HT-IR neurons in cercariae

	N in the body	*N* in each ganglia	*N* in the tail	Size in the body	Size in the tail
M. anceps	16	2	2	7.7×5.2	8.6×7.5
E. revolutum	14	2	2	5.3×2.9	3.6×2.8
C. hians	14	2	2	8.4×3.5	7.7×6.0
P. oxyurus	14	2	2	9.5×5.7	7.6×6.1
S. globulus	14	2	2	4.6×3.0	5.5×3.6
P. cervi	14	3	2	8.4×6.9	6.3×4.4
D. subclavatus	14	3	2	9.5×7.8	8.4×4.2

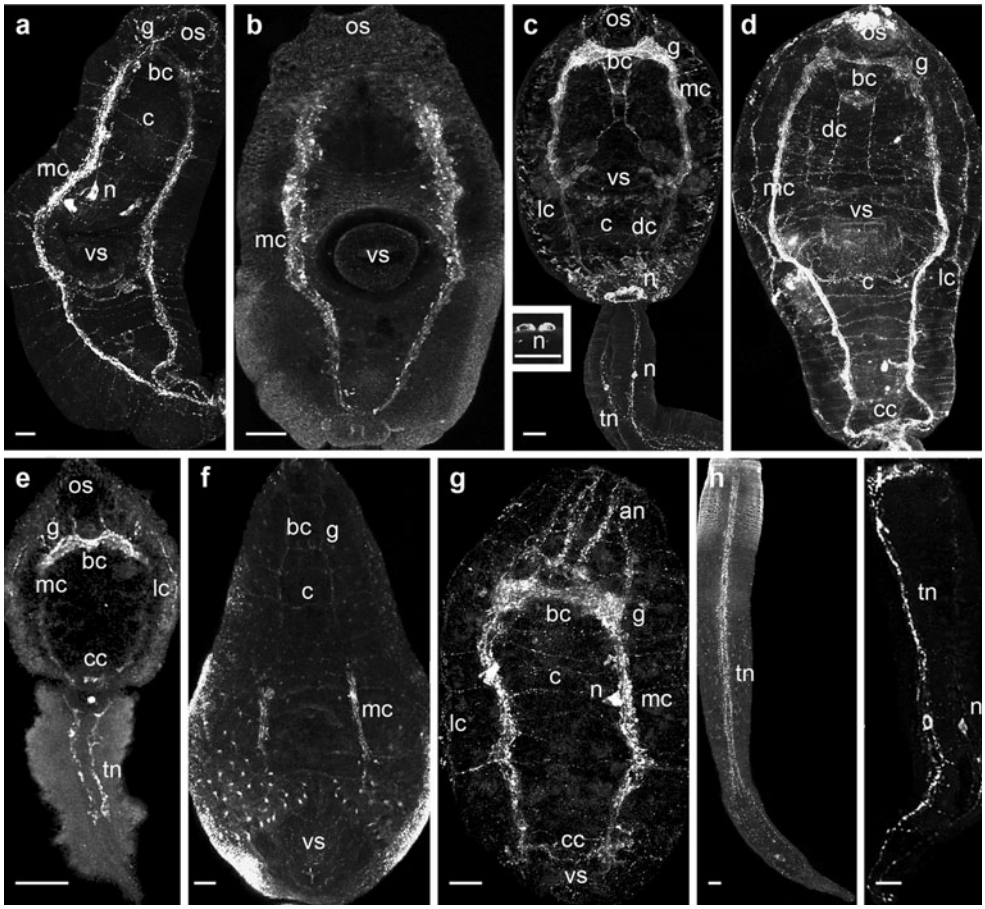

Fig. 3 **a**–**i** Confocal scanning laser micrographs of cercariae stained with anti-FMRFamide. *Bar*=20 μm. **a** Max projection showing the FMRFamide-IR nervous system in the body of *M. anceps*. Note large neurons close to ventral sucker. **b** Max projection showing the FMRFamide-IR nervous system in the body of *E. revolutum*. **c** Max projection showing the FMRFamide-IR nervous system in the body and tail of *C. hians*. *Inset* shows neurons close to bladder. **d** Max projection section showing the FMRFamide-IR nervous system in the body of *P. oxyurus*. **e** Max projection of the FMRFamide-IR nervous system in the body and tail of *S. globulus*. **f** Max projection of the FMRFamide-IR nervous system in the body of *P. cervi*. **g** Max projection of the FMRFamide-IR nervous system in the body of *D. subclavatus*. **h** Max projection of the FMRFamide-IR nervous system in the tail of *P. cervi*. **i** Max projection of the FMRFamide-IR nervous system in the tail of *M. anceps*. Note the two neurons. *an* anterior nerve, *bc* brain commissure, *cc* caudal commissure, *dc* dorsal nerve cord, *g* ganglion, *lc* lateral nerve cord, *mc* main nerve cord, *n* neuron, *os* oral sucker, *tn* tail nerve, *vs* ventral sucker

In *P. cervi* cercariae, the pattern of FMRFamide IS follows the pattern found in the other cercariae studied. The number of thin commissures in the body is 10–11. No neurons were found in the tail (Fig. 3f, h).

In cercariae *D. subclavatus*, the pattern of FMRFamide IS follows that in *P. cervi.* The number of thin commissures in the body is 14–15 (Fig. 3g). The controls were negative.

The patterns of α-tubulin immunoreactivity

In the body of *M. anceps* cercariae, α-tubulin-IR processes form a symmetrical pattern along the MCs and the minor nerve cords (Fig. 4a). The oral sucker and the armed disc are well equipped with α-tubulin-IR processes of different lengths. A few α-tubulin-IR processes were observed in the ventral sucker. The tail is covered by many α-tubulin-IR processes (Fig. 4a, Table 3).

The general distribution of α-tubulin-IR processes in the bodies of *E. revolutum*, *C. hians*, *P. oxyurus* and *S. globulus* cercariae is similar to that in *M. anceps* cercariae (Fig. 4b, c and f). The oral sucker and the armed disc of *E. revolutum* are very well equipped with α-tubulin-IR processes of different lengths (Fig. 4b). In the tail of *E. revolutum* and *C. hians*, the processes are concentrated to the first half (Fig. 4 b–d). The processes in the tail fall into two size categories, 6–7 and 2.4–3.3 μm, and they form groups (Fig. 4b, c and f; Table 3).

In the large *P. oxyurus* cercariae, only a few α-tubulin-IR processes were found, mainly concentrated around the oral sucker. In the middle of the tail of *P. oxyurus* cercariae, several α-tubulin-IR paired processes were found (Fig. 4e,

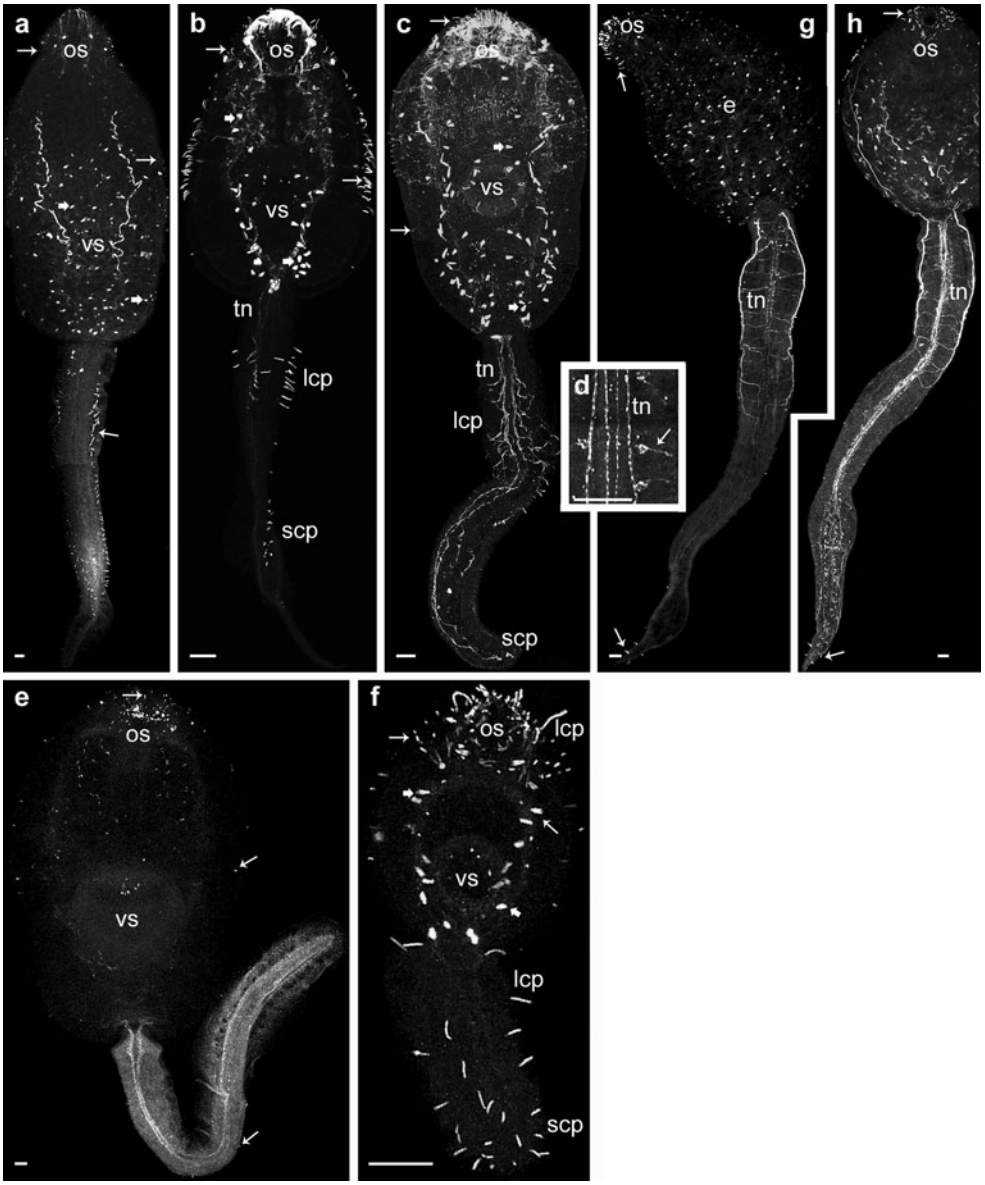

Fig. 4 **a**–**h** Confocal scanning laser micrographs of cercariae stained with anti-α-tubulin. *Bar*=20 μm. **a** Max projection showing the α-tubulin IS in *M. anceps*. **b** Max projection showing the α-tubulin IS in *E. revolutum*. **c** Max projection showing the α-tubulin IS in *C. hians*. Note the many processes on the oral sucker and armed disc and on the tail. **d** Max projection showing the α-tubulin IS processes and associated nerves in the tail of *C. hians*. **e** Max projection showing the α-tubulin IS in *P. oxyurus*. **f** Max projection showing the α-tubulin IS in *S. globulus*. Note two long processes close to the oral sucker. **g** Max projection showing the α-tubulin IS in *P. cervi*. **h** Max projection of α-tubulin IS in *D. subclavatus*. *e* encyst glands, *lcp* long ciliated processes, *os* oral sucker, *vs* ventral sucker, *scp* short ciliated processes, *tn* tail nerve, *large arrows* flame cells, *arrows* α-tubulin IS processes

Table 3). The tail has a large swimming membrane which partly hides the α-tubulin-IR processes. In *S. globulus* cercariae, a pair of long α-tubulin-IR processes (11 μm), resembling whiskers, was found on both sides of the oral sucker (Fig. 4f). In addition, many short α-tubulin-IR sensilla occur around the oral sucker. In the middle of the tail of *S. globulus*, which lacks swimming membrane, α-tubulin-IR processes of two size classes were found: six pairs of

Table 3 Length (in micrometer) and number (*N*) of α-tubulin-IR processes in the body and tail of the cercariae

	In the body	In the tail	*N* processes in the tail		
			Total	Long	Short
M. anceps	5–10	6.3–9.8	82	–	–
E. revolutum	4.3–8.8	2.4–6.9	44	22	22
C. hians	2–3	5.3–7.5	44	26	18
P. oxyurus	2–4	7–9.2	16	–	–
S. globulus	1.6–4. 11	3.9–7.0	34	12	22
P. cervi	7–8	3.5–4.5	6	–	–
D. subclavatus	1–8	1.5–4	18	4	14

long processes (5.5–7.0 μm) and ten pairs of short processes (3.9–4 μm). In the tip of the tail, two small 1-2-μm-long processes were found (Fig. 4f). In the region of the oral sucker of *P. cervi* cercariae, a bunch of α-tubulin-IR processes was observed (Fig. 4g). In the tip of the tail, six α-tubulin-IR processes are situated (Fig. 4g). In *D. subclavatus* cercariae, the distribution of α-tubulin IR processes is similar to that in *P. cervi.* In the tail, 2 pairs of long processes (4.5 μm) and 14 short processes (1.5–2 μm) were observed (Fig. 4h). The controls were negative.

Discussion

The general pattern of the phalloidin-stained F-actin filaments in body muscle fibres of the 12 cercariae studied here and in paper I is similar to that observed in other cercariae and reflects the morphology of the groups (see Halton and Maule 2004). The large variations in body size have led to variations in the musculature, the larger cercariae having larger muscle fibres (Table 1 and Table 1 in Tolstenkov et al. 2012c). Similarities between cercariae of the same size occur. In the small *S. globulus* cercariae, the lattice of muscle fibres in the body is sparse, and the striated muscle fibres in the tail do not form bundles. The pattern of muscle fibres in the body wall and in the stem of the tail of *S. globules* resembles that in the small but not related species *Skrjabinoeces similis* (Tolstenkov et al. 2012c).

The musculature of the tail shows variations which are clearly related to the different strategies of host finding. In Echinostomata, Gymnocephala and Amphistomata, which swim until they die or encyst, the striated musculature of the tail is well developed compared to Xiphidiocercariae, which have a short period of active swimming and spend the major part of their lifetime scrawling on the bottom (our observations). The cercariae of *S. globulus* are able to change the shape of their tail from short, broad and cone-shaped in the immobile position to long and narrow while swimming (our observations). The regular pattern of strictly oriented striated muscle fibres on the ventral surface of the tail may play a key role here. The variability in the organization of the tail musculature in the continuously swimming species, both the primitive and the advanced groups studied here and by Tolstenkov et al. (2012c), is small compared to that found in the intermittently swimming cercariae (Tolstenkov et al. 2011, 2012a, b).

The general neuroanatomy of the species studied corresponds to the previous studies by Mishra and Tandon (1986) and Šebelová et al. (2004). As expected, the 5-HT-IR fibres and neurons in all the 11 investigated species form orthogonal patterns that are similar to those that have been reported from cercariae of other species (see Tolstenkov et al. 2012a, b). Nine of the species studied have seven paired 5-HT-IR neurons, two species have eight. No correlation between the body size and the number of 5-HT-IR neurons could be observed (Tables 1 and 2). However, the size of the neurons follows the body size (Table 2). The number of 5-HT-IR neurons in the brain ganglia varies and increases from primitive to advanced groups (Table 4). A similar trend was observed in furcocercariae by Tolstenkov et al. (2012a, b) that represent another branch of Digenea—the Strigeidida (Gibson 1996).

No major structural differences in the FMRFamide-IR nervous systems were noticed. The number of transverse comissures in the body correlated with the size of the 11 cercariae. All species had a plexus of FMRFamide-IR nerves and neurons, forming a thick commissure in the distal part of the body where the excretory ducts open into the bladder (Tolstenkov et al. 2011, 2012a, b, c). The role of FMRFamide in the regulation of the excretory system or its musculature needs further research.

In all species, IS towards α-tubulin was observed in surface processes of different length, sensory receptors. Our results are in general agreement with the previous studies (Konstadinova 1999; Albaret et al. 1987; Zdárská 1992; Tolstenkov et al. 2011, 2012a, b). Zdárská et al. (1989) studied the ultrastructure of the tail of Echinostomata cercaria. Our data complete the picture. In the tails of all species studied, different numbers of sensory receptors were observed (Table 3). More sensory receptors were found on the tails of the primitive Echinostomata, Gymnocephala and Amphistomata than on the tails of the advanced Xiphidiocercaria (Tolstenkov et al. 2012c).

According to Haas (1994), the continuously swimming cercariae are well adapted to scan their habitats exhaustively. All species which have been found to use chemo-orientation mechanisms, such as Echinostomatidae, to locate their hosts show the continuous swimming mode of locomotion (Haas et al. 1995; Körner and Haas 1998). The distribution of α-tubulin-IR sensory receptors shows a high degree of conformity in all species studied regardless of their differences in the second intermediate host—tadpole for *C. hians* and *D. subclavatus*, mollusc for *P. oxyurus*, *S. globulus* and *M. anceps* or arthropods for the plagiorchid cercariae (Tolstenkov et al. 2012c). This indicates a similar mechanism for host finding. The *P. cervi* cercariae encyst on plants and probably have little need for chemo- or mechanoreception. The few sensory receptors are concentrated around the mouth opening and in the end of the tail.

The results of this and our earlier studies show that the NS in cercariae is conservative. However, the muscle and

Table 4 The number (*N*) of paired 5-HT-IR neurons in the brain ganglia of cercariae (papers I and II)

Family	*N* species studied	*N* neurons
Echinostomoidea	5	2
Paramphistomoidea	2	3
Plagiorchiida	4	3-4

sensory systems show variations, which are related to the host finding strategy of the species.

Acknowledgments The authors thank the staff and students of Biological Station of Belarus State University for the friendly atmosphere and help. The study was supported by RFBR grants 12-04-01051-a, 12-04-01086-a, grant of the President of Russian Federation MK-1093.2011.4, The Research Institute of the Foundation of the Åbo Akademi University and the Academy of Finland. The authors want to thank Mr. Esa Nummelin for technical assistance.

References

Albaret JL, Bayssade-Dufour C, Ngendahayo LD, Postal JM, Picot H (1987) Chaetotaxy of the cercaria of *Paramphistomum sp.*, a parasite of cattle in Vendée. Ann Parasitol Hum Comp 62:271–275

Belyakova Y (1978) New data on the life cycle of *Sphaeridiotrema globulus* Rud., 1819 (Trematoda: Psilostomidae). Life cycles, ecology and morphology of helminths of animals of Kazakhstan. Nauka, Alma-Ata, pp 192–201, in Russian

Bihovskaya-Pavlovskaya IE, Kulakova AP (1971) Cercariae of Bithyniidae snails (*Bithynia tentaculata* and *B. leachi*) from Kuronian bay. Parasitology 5:222–232 (in Russian)

Dawes B (1946) The Trematoda, with special reference to British and European forms. Cambridge University Press, Cambridge, p 644

Gibson DI (1996) Trematoda. In: Margolis L, Kabata Z (eds) Guide to the parasites of fishes of Canada. Part IV. Can Spec Publ Fish Aquat Sci 124. NRC Press, Ottawa, p 373

Ginetsinskaya TA, Dobrovolsky AA (1964) On the fauna of the larvae of trematodes from freshwater molluscs of the Volga delta. P.2. Ehinostomatid cercariae (family Echinostomatidae). Proc Astrakhan Nat Reserv 9:64–104, in Russian

Glöer P (2002) Die Süßwassergastropoden Nord- und Mitteleuropas. Bestimmungschlüssel, Lebesweise, Verbreitung. Die Tierwelt Deutschlands 73:1–237

Grabda-Kazubska B, Bayssade-Dufour C, Kiseliene V (1990) Chaetotaxy and excretory system of *Echinocercaria choanophila* U. Szidat, 1936, a larval of *Cathaemasia hians* (Rud., 1809) (Trematoda, Cathaemasiidae). Acta Parasitol Polon 35:97–105

Haas W (1994) Physiological analyses of host-finding behavior in trematode cercariae: adaptations for transmission success. Parasitology 109:15–29

Haas W, Körner M, Hutterer E, Wegner M, Haberl B (1995) Finding and recognition of the snail intermediate hosts by 3 species of echinostome cercariae. Parasitology 110:133–142

Halton DW, Maule AG (2004) Flatworm nerve-muscle: structural and functional analysis. Can J Zool 82:316–333

Herrmann KK, Sorensen RE (2011) Differences in natural infections of two mortality-related trematodes in lesser scaup and American coot. J Parasitol 97:555–558

Kanev I (1994) Life-cycle, delimitation and redescription of *Echinostoma revolutum* (Froelich, 1802) (Trematoda: Echinostomatidae). Syst Parasitol 28:125–144

Keiser J, Utzinger J (2009) Food-borne trematodiases. Clin Microbiol Rev 22:466–483

Konstadinova A (1999) Cercarial chaetotaxy of *Echinostoma miyagawai* Ishii, 1932 (Digenea: Echinostomatidae), with a review of the sensory patterns in the 'revolutum' group. Syst Parasitol 44:201–209

Körner M, Haas W (1998) Chemo-orientation of echinostome cercariae towards their snail hosts: the stimulating structure of amino acids and other attractants. Int J Parasitol 28:517–525

Mishra N, Tandon V (1986) Nervous system in *Olveria indica*, a rumen paramphistome (Digenea) of bovines, as revealed by non-specific esterase staining. J Helminthol 60:193–199

Richard J, Klein MJ, Stoeckel ME (1989) Neural and glandular localisation of substance P in *Echinostoma caproni* (Trematoda-Digenea). Parasitol Res 75:641–648

Šebelová Š, Stewart M, Mousley A, Fried B, Marks N, Halton D (2004) The musculature and associated innervation of adult and intramolluscan stages *of Echinostoma caproni* (Trematoda) visualised by confocal microscopy. Parasitol Res 93:196–206

Szidat L (1936) Uber die Entwicklungsgeschichte und den ersten Zwischenwirt von *Paramphistomum cervi* Zeder, 1790, aus dem Magen von Wiederkauern. Z Parasitenkd 9:1–19

Szidat L (1957) Life cycle of *Psilochasmus oxyurus* (Cerplin 1825, Luhe 1910) (Trematoda, Psilostomidae) in Argentina. Z Parasitenkd 18:24–35

Terenina NB, Tolstenkov OO, Fagerholm HP, Serbina EA, Vodjanizkaya SN, Gustafsson MKS (2006) The spatial relationship between the musculature and the NADPH-diaphorase activity, 5-HT and FMRFamide immunoreactivities in redia, cercaria and adult *Echinoparyphium aconiatum* (Digenea). Tissue Cell 38:151–157

Tolstenkov OO, Terenina NB, Gustafsson MKS, Serbina EA, Kreshchenko ND, Maklakova LM, Jashina AV (2008) Immunochemical study of cercariae trematodes from different taxonomic groups—a preliminary study. Acta Biol Hung 59: S221–S225

Tolstenkov OO, Prokofiev VV, Terenina NB, Gustafsson MKS (2011) The neuro-muscular system in cercaria with different patterns of locomotion. Parasitol Res 108:1219–1227

Tolstenkov OO, Akimova LN, Chrisanfova GG, Terenina NB, Gustafsson MKS (2012a) The neuro-muscular system in fresh-water furcocercaria from Belarus. I Schistosomatidae. Parasitol Res 110:185–193

Tolstenkov OO, Akimova LN, Chrisanfova GG, Terenina NB, Gustafsson MKS (2012b) The neuromuscular system in freshwater furcocercaria from Belarus. II Diplostomidae, Strigeidae and Cyathocotylidae. Parasitol Res 110:583–592

Tolstenkov OO, Akimova LN, Terenina NB, Gustafsson MKS (2012c) The neuromuscular system in continuously swimming cercariae from Belarus. I Xiphidiocercariae. Parasitol Res. doi:10.1007/s00436-012-3044-1

Zdárská Z (1992) Transmission electron microscopy of sensory receptors of *Echinostoma revolutum* (Froelich 1802) cercaria (Digenea: Echinostomatidae). Parasitol Res 78:598–606

Zdárská Z, Nasincová V, Valkounová J (1989) Ultrastructure of the tail of *Echinostoma revolutum* cercaria. Folia Parasitol 36(3):239–242